NACA

RESEARCH MEMORANDUM

COMPARISON WITH THEORY OF LANDING IMPACTS OF A MODEL

OF A SEAPLANE INCORPORATING A HYDRO-SKI

WITH AND WITHOUT A SHOCK ABSORBER

By Edward L. Hoffman

Langley Aeronautical Laboratory
Langley Field, Va.

CLASSIFICATION CHANGED

UNCLASSIFIED

To_____

NACA Res Abs

By authority of_____ Date_____
$V R N · 126$ effective Apr. 15. 1958
AMT 5·12·58

NATIONAL ADVISORY COMMITTEE
FOR AERONAUTICS
WASHINGTON
July 11, 1956

NATIONAL ADVISORY COMMITTEE FOR AERONAUTICS

RESEARCH MEMORANDUM

COMPARISON WITH THEORY OF LANDING IMPACTS OF A MODEL

OF A SEAPLANE INCORPORATING A HYDRO-SKI

WITH AND WITHOUT A SHOCK ABSORBER

By Edward L. Hoffman

SUMMARY

Experimental data from calm- and rough-water landing impacts were
obtained in Langley tank no. 2 with a dynamic model of a seaplane incor-
porating a flat-bottom hydro-ski mounted on a rigid strut and on a
shock-absorber strut so that the ski translated normal to its keel with-
out changing trim. Theoretical computations based on the application
of planing data to the impact conditions have been made and compared with
the experimental data. The method used for the calm-water rigid-strut
computations was obtained from NACA Technical Note 2814 and the method
for the shock-absorber strut in calm water, from NACA Research
Memorandum L54H10. In order to adapt these basic methods to cover the
rough-water case, a method was developed for obtaining an equivalent
wave slope on which to base computations instead of the slope of the
wave at the initial point of contact. Computed results for both rigid
struts and shock-absorber struts are compared with experimental data in
time-history plots and are in good agreement for both calm-water and
rough-water impacts.

INTRODUCTION

A method for determining water landing impact loads on rigidly
mounted planing surfaces by the application of steady-planing forces
has been reported in reference 1 and has been shown to be applicable to
water landing impacts of a rigidly mounted flat-plate V-step hydro-ski
in reference 2. A method for determining water landing impact forces of
shock-absorber-mounted translating hydro-skis has been reported in
reference 3.

The present report shows the applicability of these methods to calm- and rough-water landing impacts of a dynamic model of a seaplane having either a fixed or translating flat-bottom hydro-ski. The experimental data were obtained in an extension of the tests reported in reference 4 and the model used was the same.

SYMBOLS

A cross-sectional area of shock strut

b beam of ski

C_B planing-lift coefficient, $\dfrac{F_p}{\rho/2 \; \dot{x}^2 b^2}$

$C_B' = \dfrac{C_B}{1 + \dfrac{m_w}{m}}$

$C_\triangle$ beam-loading coefficient of ski, $\dfrac{m}{\rho b^3}$

c damping constant of shock strut

F force

g acceleration due to gravity

H wave height measured from trough to crest

k generalized draft coefficient, $\dfrac{1}{2C_\triangle \sin^2\tau \cos^2\tau} \displaystyle\int_0^{z/b} C_B' \, d\frac{z}{b}$

L wave length measured from crest to crest

m mass of model

m_w virtual mass of water

n damping exponent

r_s rise of ski normal to undisturbed or calm-water surface relative to its position at water contact

V	resultant velocity
v	air volume of shock strut
$\dot{x}$	velocity of ski parallel to undisturbed water surface
$\dot{x}_\alpha$	advancing velocity of trochoidal wave, $\sqrt{\dfrac{gL}{2\pi}}$
z	draft (vertical displacement of ski trailing edge relative to water surface)
$\dot{z}$	velocity of ski normal to undisturbed water surface
$\ddot{z}$	acceleration of ski normal to undisturbed water surface
γ	flight-path angle relative to undisturbed water surface
ϵ	impact parameter, $\dfrac{\tan(\gamma_0 + \tau)}{\tan \tau}$
θ	angle of inclination of water surface
κ	approach parameter, $\dfrac{\sin \tau}{\sin \gamma_0} \cos\!\left(\tau + \gamma_0\right)$
ρ	mass density of water
τ	trim of ski relative to undisturbed water surface
$\psi(\omega)$	psi function, $\dfrac{1}{\omega} + \log_e \omega - 1$

Subscripts:

a	pneumatic, shock absorber
e	effective (referred to inclined water surface instead of undisturbed water surface)
h	hydraulic, shock absorber
o	time of initial water contact
p	planing, ski
l	relative to wave particles at selected part of wave
W	wave-particle velocity

Superscript:

'   referred to fuselage of model instead of to ski

APPARATUS AND PROCEDURE

Experimental data for this investigation were obtained from free-to-trim landing tests of Langley tank model 280, which is a 1/24-scale dynamic model of a 160,000-pound seaplane design equipped with a hydro-ski. The tests were conducted from the main carriage fore-and-aft gear in Langley tank no. 2. The test conditions are given in table I, a photograph of the model and gear is shown in figure 1, and a drawing of the hydro-ski is shown in figure 2. The ski was attached to the hull by two rigid struts for fixed-ski tests and by a shock-absorber strut so that the ski moved normal to its keel without changing trim (fig. 3) for translating-ski tests.

For landing tests with the fore-and-aft gear, the model had approximately 3 feet of fore-and-aft freedom with respect to the towing carriage in order to absorb longitudinal accelerations introduced by impacts and to permit the model to act as a free body in the longitudinal direction. The model was free to trim about a pivot located at the center of gravity and was free to move vertically, but was restrained in roll and yaw.

To make a landing test with this gear the towing carriage was brought up to a speed sufficient to make the model fly. An electrically actuated trim lock, which was attached to the towing staff, fixed the trim of the model in the air during the landing approach and was automatically released when the model touched the water.

In order to land the model, the carriage was decelerated at a constant rate so the model glided to the water. The carriage deceleration was selected to keep the model between the fore-and-aft limits of travel during the landing.

A recording oscillograph located in the towing carriage was used to record data. A strain-gage type of accelerometer mounted on the towing staff of the model was used to measure vertical accelerations. The natural frequencies of the accelerometer and recording galvanometer were 165 cps and 150 cps, respectively. Both were damped to about 65 percent of critical damping. Slide-wire pickups were used to measure trim, rise, and fore-and-aft position of the model and to measure deflection of the shock strut.

Figure 4 is a detailed drawing of the shock-absorber strut. The maximum shock-absorber stroke was 1 inch, the initial air pressure 51 pounds per square inch, and the air volume ratio 3 to 1. The characteristics of the shock absorber were obtained from bench-tests and are presented in figure 5. Figure 5(a) is a plot of pneumatic force against stroke and figure 5(b) is a plot of the stroke obtained from drop tests of various heights. The weight used for the drop tests was equal to the gross weight of the model. The variation of hydraulic force with telescoping velocity was obtained from the drop tests and is shown in figure 5(c).

Distilled water was used in the strut instead of shock-absorber fluid in order to increase the Reynolds number of the flow through the orifice so that the flow would be turbulent as is the case with the full-scale shock absorber. With the model shock absorber the flow was considered turbulent $\left(F_h \text{ varies as } (\dot{z}' - \dot{z})^2\right)$ above telescoping velocities of 1.5 feet per second, but was considered laminar (viscous damping where F_h varies as $(\dot{z}' - \dot{z})$) below telescoping velocities of 1.5 feet per second. (See fig. 5(c).) In the model tests, telescoping velocities below 1.5 feet per second were obtained for calm-water landings and telescoping velocities above 1.5 feet per second were obtained for landings in waves.

The Langley tank no. 2 wave machine was used to produce the rough-water conditions. In order to obtain wave profile records, two lightweight floats were mounted as near the center line of the tank as feasible on pivoted beams and data were transmitted through slide-wire pickups to a recording oscillograph. A drawing of the wave-recorder setup is shown in figure 6. By using two floats, wave lengths and velocities were obtainable as well as wave heights.

To obtain the model position relative to the waves, a wave prod was mounted on the towing carriage (fig. 1) to record the wave-crest location while contact points installed at the leading and trailing edges of the hydro-ski recorded the model position. The model position relative to the waves was also checked by rise measurements and by longitudinal measurements from the wave recorder station.

The planing data necessary for the computational procedures were obtained from a brief test using the small-model towing gear in Langley tank no. 2. The hydro-ski (fig. 2) was tested at trims of 4°, 8°, and 12° at various drafts and speeds. Lift and speed were recorded and underwater photographs were taken to obtain wetted areas. These data are presented as a plot of planing lift coefficient against generalized draft (fig. 7).

METHOD OF CALCULATION

The equations used to compute the impact loads and motions were derived from reference 1 for the fixed-ski configuration and from reference 3 for the translating-ski configuration. Both computational procedures used were based on the application of planing data to the impact conditions and are described in detail in the appendix. It was assumed that the model remained fixed in trim, and had a wing lift force equal to the model weight throughout the impacts. With the relatively high beam loading of the hydro-ski ($C_\triangle = 16.8$), the virtual mass of the water was assumed to be a small part of the total mass involved and was neglected. In order to adapt the basic methods of references 1 and 3 to the rough-water case the initial landing conditions were referred to the slope and velocity increments of the waves.

The assumed water surface used for theoretical computations was an inclined plane with the slope equal to the slope at the initial point of ski contact of a trochoidal wave having the same height and length as the experimental wave. Inasmuch as the inclined plane varies from the experimental wave profiles, some discrepancies in vertical accelerations and draft are to be expected prior to the experimental wave crest. This variation was especially true for relatively short waves. It was suggested in reference 5 that, for computing rough-water impacts, a slope of the wave encountered at some point during the impact should be used instead of the slope at the point of initial contact. The maximum acceleration was of primary interest; therefore, it seemed deducible that the location of an equivalent slope should be related to the time that peak acceleration occurred. The time of the peak acceleration from calculations based on the initial contact slope was used to compute a horizontal displacement (based on $\dot{x}_0 + \dot{x}_\alpha$) of the ski relative to the trochoidal wave. This horizontal displacement from the initial point of contact located a tangent to the trochoidal wave surface that was used as the equivalent slope. The equivalent wave slope and the wave velocities at that point were then used to obtain a new set of initial landing conditions.

It should be noted that the assumed water surface (either contact slope or equivalent slope) does not even approximate the experimental wave profile after the wave crest is reached and comparison between theory and experiment should not be considered.

The velocity increments due to wave motion were introduced in the initial landing conditions by using the orbital velocities of the water particles at the selected part of the wave. If the hydro-ski motion is referred to the wave (see fig. 8) the relative horizontal and vertical velocities become

$$\dot{x}_l = \dot{x} + \dot{x}_W \tag{1}$$

$$\dot{z}_l = \dot{z} + \dot{z}_W \tag{2}$$

where $\dot{x}_W$ and $\dot{z}_W$ are computed for the selected part of a trochoidal wave having the same height and length as the wave the model contacted. The resultant ski velocity is

$$V_l = \sqrt{\dot{x}_l{}^2 + \dot{z}_l{}^2} \tag{3}$$

The flight-path angle relative to the inclined water surface is

$$\gamma_e = \theta + \gamma_l = \theta + \tan^{-1} \frac{\dot{z}_l}{\dot{x}_l}$$

where θ is the wave slope under consideration. The ski velocity normal to the water surface is

$$\dot{z}_e = V_l \sin \gamma_e \tag{5}$$

RESULTS AND DISCUSSION

The experimental results and comparison with theory are presented as time histories of vertical accelerations and motions for fixed-ski cases in figure 9 and of vertical accelerations, motions, and shock-absorber stroke for translating-ski cases in figure 10. The theoretical results presented for the landings in waves were obtained with the equivalent-slope method. One typical example where computations were based on the contact slope is presented for comparison.

Fixed-Ski Case

Time histories of draft and vertical acceleration are shown in figure 9(a) for a calm-water impact with a fixed hydro-ski. The draft plot shows the path of the hydro-ski trailing edge relative to the undisturbed water surface. The maximum draft is underestimated by the theory by about 14 percent of the experimental value and is displaced in time somewhat whereas the theoretical vertical accelerations show very good agreement with experiment. Figures 9(b) and 9(c) are examples of impacts in waves approximately 3 inches high. A rise plot is presented, in

addition to the draft plot, in order to show the path of the ski through the waves. Figure 9(b) is for a landing impact on the flank of a relatively short wave $\left(\text{approximately } 2\frac{1}{2} \text{ times the hull length}\right)$ and shows theoretical results obtained from computations based on the contact wave slope and on the equivalent wave slope. The time histories of vertical acceleration (terminated where the hull afterbody contacted the wave) show that the maximum computed value based on the contact wave slope is about 22 percent higher than the experimental maximum, whereas the computed value based on the equivalent wave slope is about 12 percent higher than the experimental maximum. The theoretical plots of draft and rise are approximately the same and both are in good agreement with the experimental values until the wave crest is reached. The maximum theoretical draft occurs after the wave crest is reached, but if the draft at the wave crest were assumed to be the maximum value, it would be within 10 percent of the experimental maximum.

Figure 9(c) is an example of a landing impact on the flank of a relatively long wave (approximately 5 times the hull length). The theoretical values of vertical accelerations, based on the equivalent wave slope, closely approximate the experimental values. The theoretical draft plot is also in good agreement with experiment until the wave crest is reached as was the case in figure 9(b). The theoretical maximum draft is attained before the experimental wave crest is reached and, although it is displaced in time somewhat, the maximum value is within 10 percent of the maximum experimental value.

Translating-Ski Case

Time histories of draft, vertical accelerations and stroke for a calm-water impact with the hydro-ski mounted on a shock-absorber strut are given in figure 10(a) and show reasonably good agreement between theory and experiment. The discrepancies that do exist are attributed to the difficulty of obtaining the experimental shock-absorber data necessary for substitution in the theory when such a short shock-absorber stroke is involved. Figures 10(b) and 10(c) are plots of impacts in waves approximately 3 inches high using the shock-absorber mounted hydro-ski.

Figure 10(b) is for a wave length approximately $2\frac{1}{2}$ times the hull length. The plot of vertical accelerations (terminated where the hull afterbody contacted the wave) shows that the theoretical values of vertical acceleration agree very well with the experiment. The theoretical plots of stroke, draft, and rise are in reasonable agreement with experiment until the experimental wave crest is reached.

In figure 10(c), for a wave length approximately 5 times the hull length, the theoretical plots of vertical acceleration, stroke, and draft

closely approximate the experimental plots. In figures 10(b) and (c) the maximum theoretical values of stroke and draft occur after the experimental wave crest is reached. If the theoretical values at the crest were considered maximums the stroke and draft from figure 10(c) and the draft from figure 10(b) would be within 5 percent of the experimental maximums, but the stroke from figure 10(b), which is for a landing in a wave only $2\frac{1}{2}$ times the hull length, would be overestimated about 27 percent.

CONCLUDING REMARKS

Comparison of theory with experiment showed good agreement for both fixed- and translating-ski cases for calm-water impacts and for rough-water impacts until the experimental wave crest was reached. In some cases the peak theoretical values of draft and shock-absorber stroke were not obtained prior to the wave crest, but if the values at the wave crest are used as maximum values they will agree reasonably well with experimental maximums even in waves as short as $2\frac{1}{2}$ times the hull length.

Langley Aeronautical Laboratory,
    National Advisory Committee for Aeronautics,
        Langley Field, Va., April 11, 1956.

APPENDIX

COMPUTATIONAL PROCEDURES

Fixed-Ski Case

The basic equations, obtained from references 1 and 2, used to compute loads and motions for the fixed-ski case are

$$-\ddot{z} = \frac{\rho b^2 V_0{}^2 \cos^2(\gamma_0 + \tau)}{2m \cos^2 \tau} C_B{}' \left\{ \psi^{-1}\left[\psi(\epsilon) - k\right] \right\}^2 \tag{A1}$$

and

$$\dot{z} = \frac{\dot{z}_0}{\epsilon - 1}\left\{ \psi^{-1}\left[\psi(\epsilon) - k\right] - 1 \right\} \tag{A2}$$

where

$$k = \frac{1}{2C_\triangle \sin^2 \tau \cos^2 \tau} \int_0^{z/b} C_B{}' d\frac{z}{b}$$

Inasmuch as the virtual mass of the water is being neglected, in the equation

$$C_B{}' = \frac{C_B}{1 + \dfrac{m_w}{m}} \tag{A3}$$

the modified planing coefficient $C_B{}'$ is considered to equal C_B. The values of C_B required for the computations were obtained from the planing tests of the hydro-ski.

For calculating the generalized draft coefficient k it was necessary to integrate the plot of C_B against z/b. Inasmuch as integration of equations was simpler than graphical integration, straight-line segments were substituted for the curves of C_B against z/b as shown in figure 7.

For impacts that submerged the bow of the hydro-ski, the planing coefficient was assumed to be a constant value beyond the draft that

would submerge a rectangular flat plate of equivalent length of the hydro-ski. This assumption is reasonable because the ski submerged very little (only at wave crests) and because a ski submerging under impact conditions would have a bubble type of ventilated flow over the upper surface that would not contribute additional lift. By considering a constant value for C_B after the bow submerged, an example of the equation from figure 7 for a landing trim of $4°$ would be

$$C_B = 0.667z/b \qquad (z/b < 0.094) \qquad (A4)$$

$$C_B = 0.122z/b + 0.0511 \qquad \left(z/b \begin{array}{c} > 0.094 \\ < 0.280 \end{array}\right) \qquad (A5)$$

$$C_B = 0.0853 \qquad (z/b > 0.280) \qquad (A6)$$

Interpolation of the data of figure 7 gave the necessary planing-coefficient equations for the specific landing trims of the test conditions.

The impact loads and motions of the model were computed in the following manner: A series of values of z/b were chosen. The corresponding values of C_B were then computed from equations such as (A4), (A5), and (A6) obtained from figure 7. The C_B values and the initial landing conditions were then used in equations (A1) and (A2) to obtain solutions for vertical velocity and acceleration. The necessary ψ-function values are listed in table II as obtained from reference 1. The vertical velocity and acceleration "draft histories" were converted to time histories by integration of a plot of $1/\dot{z}$ against z until, as $\dot{z}$ approaches 0, values of $1/\dot{z}$ became too large. The time history was continued by integration of a plot of $1/\ddot{z}$ against $\dot{z}$ until $\dot{z}$ became large enough to continue integration of the rebound part of the plot of $1/\dot{z}$ against z.

Translating-Ski Case

The basic equations, derived from reference 3, used to compute loads and motions for the translating-ski case are

$$\ddot{z}' + \frac{(\dot{z} + \kappa \dot{z}_0)^2 F_p}{bC_\Delta \cos^2\tau \rho b^2 \dot{x}^2 \sin^2\tau} = 0 \qquad (A7)$$

and

$$\ddot{z}' \pm \frac{c(\pm\dot{z}' \mp \dot{z})^n}{m \cos^{n-1}\tau} + \frac{F_a \cos \tau}{m} = 0 \tag{A8}$$

Equation (A7) was obtained from equations (5), (11), and (12) of reference 3 and equation (A8) was obtained from equation (6) of reference 3. These equations neglect the mass of the ski and lower part of the shock strut, because they are a small part of the total mass involved. The friction force of the shock strut is also neglected. The planing force F_p is obtained from the planing-lift-coefficient equation of figure 7 in the same manner as for the fixed-ski case. The pneumatic force F_a of the shock absorber is obtained from the equation

$$F_a = \frac{F_{a_0} v_0}{v_0 - A(z' - z)} = \frac{11.25}{1.5 - (z' - z)} \tag{A9}$$

which is based on the initial strut pressure and the physical dimensions of the strut, with the strut air compression considered isothermal. A comparison of equation (A9) and the experimental pneumatic force is shown in figure 5(a). The damping constant c and the damping exponent n were obtained from figure 5(c) which is a plot of hydraulic force against telescoping velocity that was obtained from drop tests of the shock absorber. For strut telescoping velocities below 1.5 feet per second the damping force was considered to vary directly as the telescoping velocity ($n = 1$) and above 1.5 feet per second the damping force was considered to vary as the square of the telescoping velocity ($n = 2$). From these data and values of initial landing conditions, solutions of equations (A7) and (A8) were made on an electronic analog computer.

Fixed-ski cases can be obtained from the electronic analog computer by using equation (A7) inasmuch as equation (A8) does not apply when the strut is considered rigid. Under such conditions equation (A7) can be shown to equal equation (A1).

REFERENCES

1. Smiley, Robert F.: The Application of Planing Characteristics to the Calculation of the Water-Landing Loads and Motions of Seaplanes of Arbitrary Constant Cross Section. NACA TN 2814, 1952.

2. Miller, Robert W.: Water Landing Investigation of a Flat-Bottom V-Step Model and Comparison With a Theory Incorporating Planing Data. NACA TN 2932, 1953.

3. Schnitzer, Emanuel: Water-Impact Theory for Aircraft Equipped With Nontrimming Hydro-Skis Mounted on Shock Struts. NACA RM L54H10, 1954.

4. Hoffman, Edward L, and Fisher, Lloyd J.: Model Investigation of the Effect of Mounting Hydro-Skis on Shock Absorbers. NACA RM L54L02, 1955.

5. Miller, Robert W.: Hydrodynamic Impact Loads in Rough Water for a Prismatic Float Having an Angle of Dead Rise of 30°. NACA TN 1776, 1948.

TABLE I.- INITIAL LANDING CONDITIONS

$$\left[C_\triangle = 16.8\right]$$

Case	τ, deg	$\dot{x}$, ft/sec	$\dot{z}$, ft/sec	γ, deg	H, in.	L, in.	θ, deg	τ_e, deg	V_l, ft/sec	γ_e, deg
Fixed-ski	9.8	49.5	1.30	1.50	Calm		0			
	9.1	54.4	1.65	1.75	3.18	114	5.0 contact slope	4.1	54.5	7.4
							4.5 equivalent slope	4.62	54.5	6.80
	9.8	52.7	1.66	1.81	2.94	220	1.65 equivalent slope	8.15	53.0	3.76
Translating-ski	9.4	49.9	1.2	1.38	Calm		0	.		
	8.9	54.7	1.96	2.05	2.58	118	3.54 equivalent slope	5.40	54.9	6.06
	9.0	54.7	1.71	1.79	2.96	218	1.76 equivalent slope	7.24	55.0	3.86

TABLE II.- ψ-FUNCTION

$$\psi(\omega) = \frac{1}{\omega} + \log_e \omega - 1$$

| ω	ψ(ω)	ω	ψ(ω)	ω	ψ(ω)	ω	ψ(ω)	ω	ψ(ω)	ω	ψ(ω)	ω	ψ(ω)	ω	ψ(ω) (a)
0.01	94.3948	0.41	0.5474	0.81	0.0239	1.21	0.0171	1.61	0.0973	2.01	0.1956	2.41	0.2946	2.81	0.3891
.02	45.0880	.42	.5135	.82	.0210	1.22	.0185	1.62	.0997	2.02	.1982	2.42	.2970	2.82	.3914
.03	28.8267	.43	.4816	.83	.0185	1.23	.0200	1.63	.1021	2.03	.2007	2.43	.2994	2.83	.3936
.04	20.7811	.44	.4517	.84	.0161	1.24	.0216	1.64	.1045	2.04	.2032	2.44	.3018	2.84	.3959
.05	16.0043	.45	.4237	.85	.0140	1.25	.0231	1.65	.1068	2.05	.2056	2.45	.3043	2.85	.3982
.06	12.8533	.46	.3974	.86	.0120	1.26	.0248	1.66	.1092	2.06	.2082	2.46	.3067	2.86	.4005
.07	10.6264	.47	.3727	.87	.0101	1.27	.0264	1.67	.1116	2.07	.2106	2.47	.3091	2.87	.4027
.08	8.9742	.48	.3493	.88	.0086	1.28	.0281	1.68	.1140	2.08	.2131	2.48	.3115	2.88	.4050
.09	7.7032	.49	.3275	.89	.0071	1.29	.0298	1.69	.1165	2.09	.2156	2.49	.3139	2.89	.4073
.10	6.6974	.50	.3068	.90	.0057	1.30	.0316	1.70	.1189	2.10	.2181	2.50	.3163	2.90	.4095
.11	5.8836	.51	.2875	.91	.0046	1.31	.0334	1.71	.1213	2.11	.2206	2.51	.3187	2.91	.4118
.12	5.2130	.52	.2692	.92	.0036	1.32	.0352	1.72	.1237	2.12	.2231	2.52	.3211	2.92	.4141
.13	4.6521	.53	.2519	.93	.0027	1.33	.0371	1.73	.1262	2.13	.2256	2.53	.3235	2.93	.4163
.14	4.1768	.54	.2357	.94	.0019	1.34	.0389	1.74	.1286	2.14	.2281	2.54	.3259	2.94	.4186
.15	3.7696	.55	.2204	.95	.0013	1.35	.0408	1.75	.1311	2.15	.2306	2.55	.3283	2.95	.4208
.16	3.4174	.56	.2059	.96	.0009	1.36	.0428	1.76	.1335	2.16	.2331	2.56	.3306	2.96	.4230
.17	3.1104	.57	.1923	.97	.0004	1.37	.0447	1.77	.1360	2.17	.2356	2.57	.3330	2.97	.4253
.18	2.8408	.58	.1794	.98	.0002	1.38	.0467	1.78	.1384	2.18	.2380	2.58	.3354	2.98	.4275
.19	2.6025	.59	.1673	.99	.0000	1.39	.0487	1.79	.1409	2.19	.2405	2.59	.3378	2.99	.4297
.20	2.3906	.60	.1559	1.00	.0000	1.40	.0508	1.80	.1434	2.20	.2430	2.60	.3401	3.00	.4319
.21	2.2013	.61	.1450	1.01	.0001	1.41	.0528	1.81	.1458	2.21	.2455	2.61	.3425	3.10	.4540
.22	2.0314	.62	.1349	1.02	.0002	1.42	.0549	1.82	.1483	2.22	.2480	2.62	.3449	3.20	.4757
.23	1.8781	.63	.1253	1.03	.0004	1.43	.0570	1.83	.1508	2.23	.2504	2.63	.3472	3.30	.4970
.24	1.7296	.64	.1162	1.04	.0007	1.44	.0591	1.84	.1534	2.24	.2529	2.64	.3496	3.40	.5179
.25	1.6137	.65	.1077	1.05	.0012	1.45	.0612	1.85	.1557	2.25	.2554	2.65	.3519	3.50	.5385
.26	1.4991	.66	.0997	1.06	.0017	1.46	.0634	1.86	.1582	2.26	.2578	2.66	.3543	3.60	.5587
.27	1.3944	.67	.0920	1.07	.0022	1.47	.0655	1.87	.1607	2.27	.2603	2.67	.3566	3.70	.5786
.28	1.2984	.68	.0849	1.08	.0029	1.48	.0677	1.88	.1632	2.28	.2628	2.68	.3590	3.80	.5982
.29	1.2104	.69	.0782	1.09	.0036	1.49	.0699	1.89	.1657	2.29	.2652	2.69	.3613	3.90	.6174
.30	1.1293	.70	.0719	1.10	.0044	1.50	.0721	1.90	.1682	2.30	.2677	2.70	.3636	4.00	.6363
.31	1.0546	.71	.0660	1.11	.0053	1.51	.0744	1.91	.1707	2.31	.2702	2.71	.3660	4.10	.6549
.32	.9856	.72	.0604	1.12	.0062	1.52	.0766	1.92	.1732	2.32	.2726	2.72	.3683	4.20	.6732
.33	.9216	.73	.0552	1.13	.0072	1.53	.0789	1.93	.1757	2.33	.2751	2.73	.3706	4.30	.6912
.34	.8624	.74	.0503	1.14	.0082	1.54	.0811	1.94	.1782	2.34	.2775	2.74	.3729	4.40	.7089
.35	.8073	.75	.0456	1.15	.0093	1.55	.0834	1.95	.1807	2.35	.2800	2.75	.3752	4.50	.7263
.36	.7562	.76	.0414	1.16	.0105	1.56	.0857	1.96	.1831	2.36	.2824	2.76	.3776	4.60	.7435
.37	.7084	.77	.0373	1.17	.0117	1.57	.0880	1.97	.1856	2.37	.2848	2.77	.3799	4.70	.7603
.38	.6640	.78	.0336	1.18	.0130	1.58	.0903	1.98	.1882	2.38	.2873	2.78	.3822	4.80	.7770
.39	.6225	.79	.0301	1.19	.0143	1.59	.0927	1.99	.1906	2.39	.2897	2.79	.3845	4.90	.7933
.40	.5837	.80	.0269	1.20	.0156	1.60	.0950	2.00	.1932	2.40	.2921	2.80	.3868	5.00	.8094
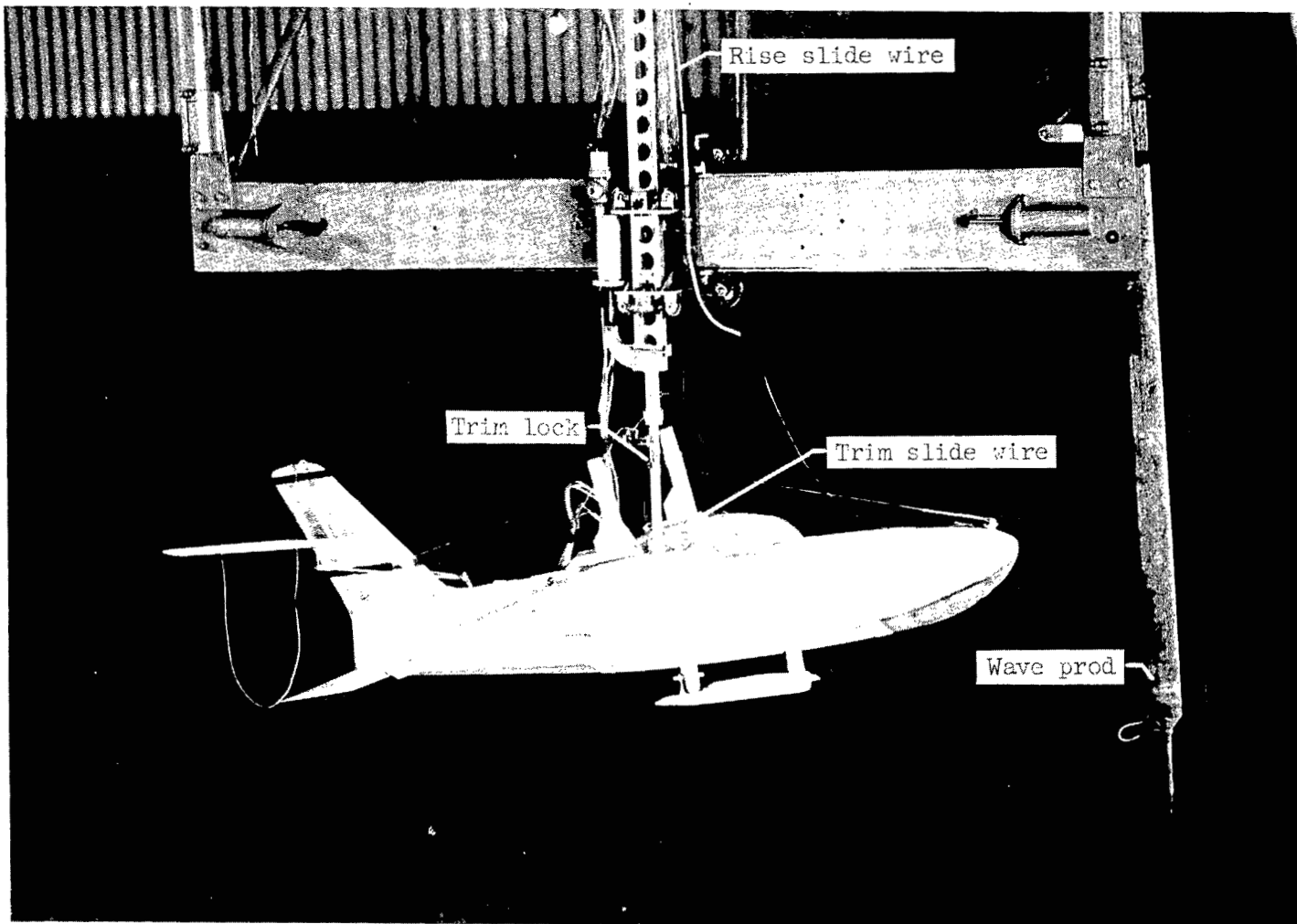
Figure 1.- Langley tank model 280 on fore-and-aft gear. L-81784.1
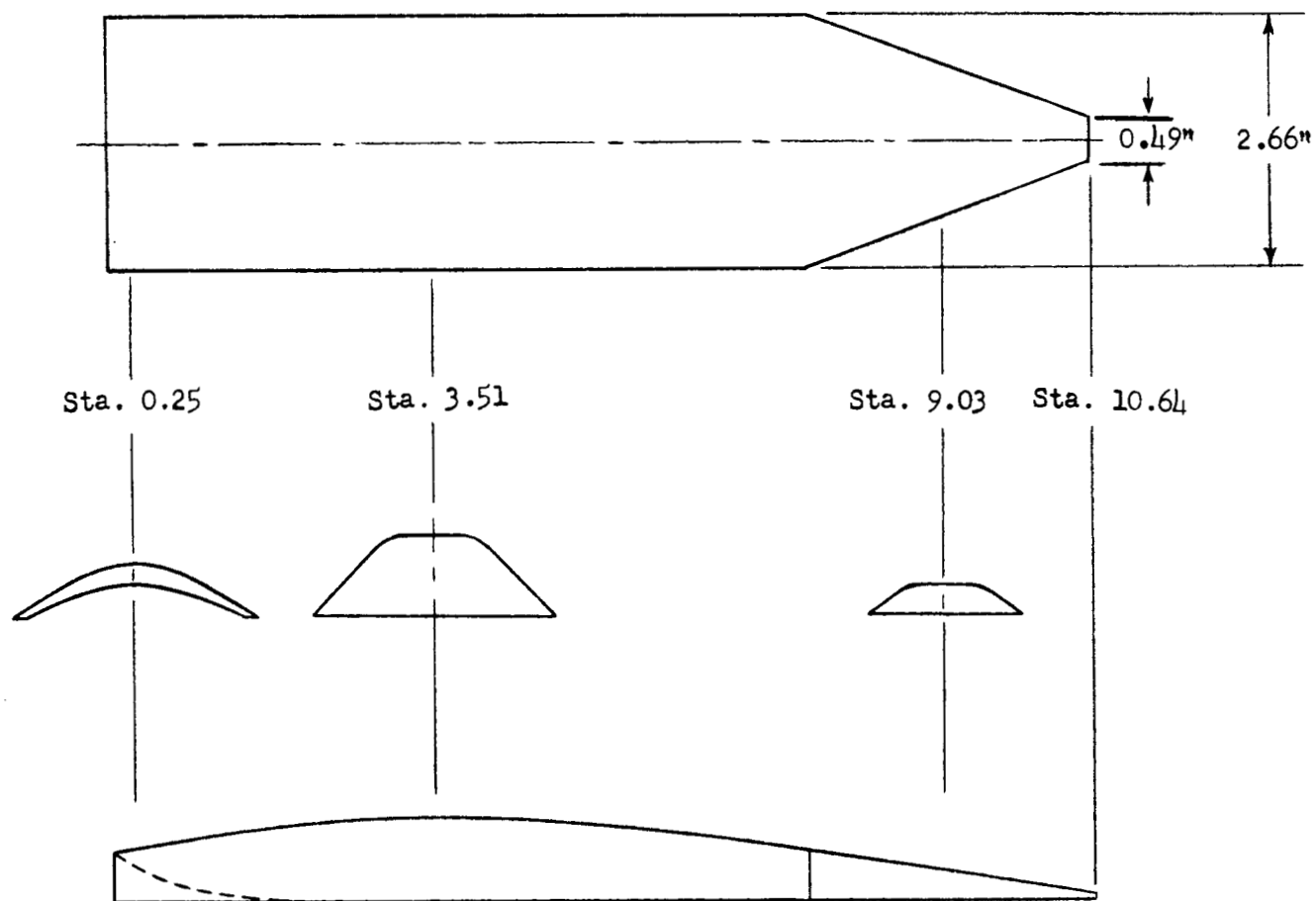
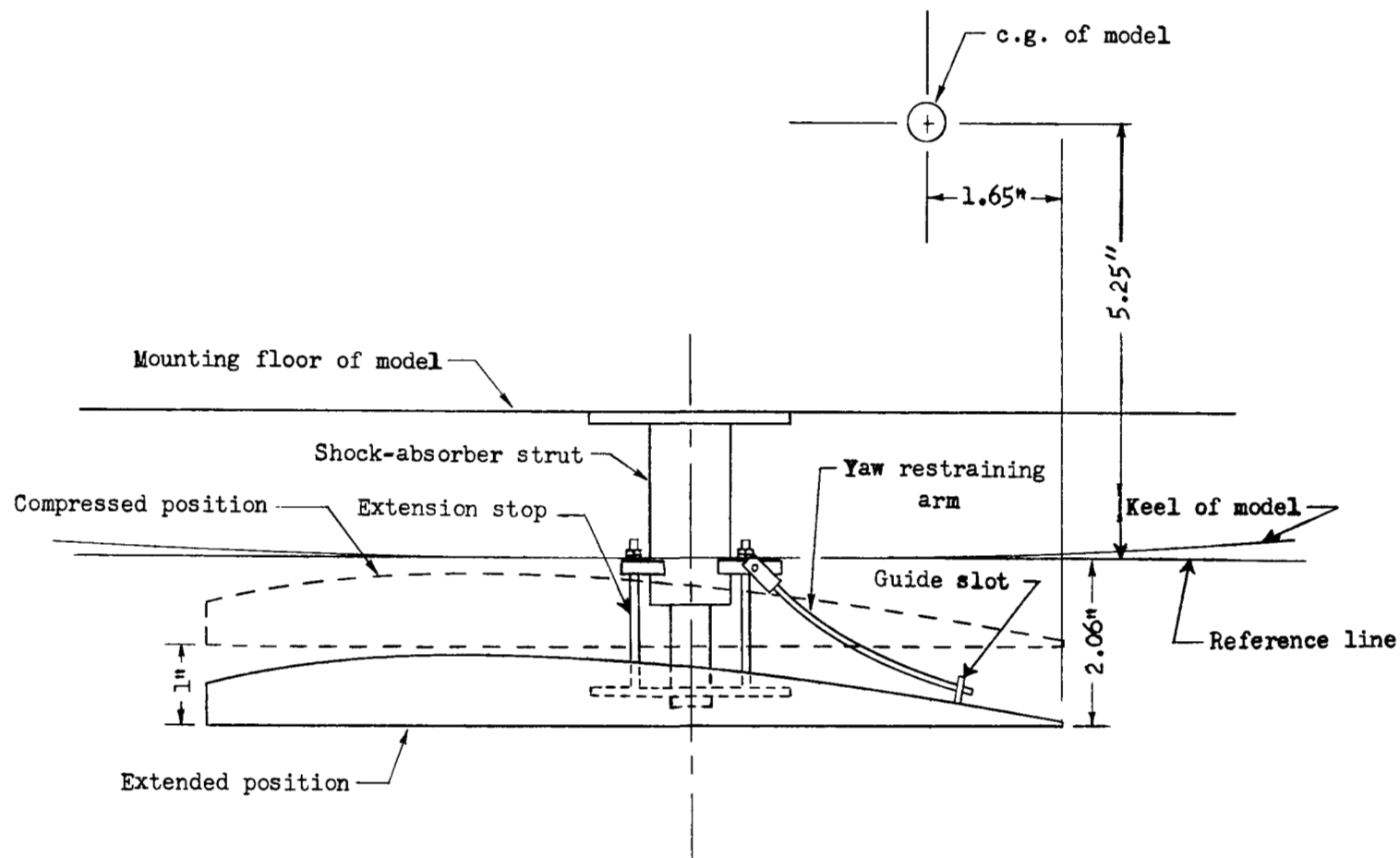Figure 2.- Flat-bottom hydro-ski of Langley tank model 280.

c.g. of model

←—1.65"—→

5.25"

Mounting floor of model

Shock-absorber strut

Yaw restraining arm

Compressed position

Extension stop

Keel of model

Guide slot

2.06"

Reference line

1"

Extended position

Figure 3.- Translating hydro-ski strut configuration.

Air valve

Piston

Hull mounting bracket

Linear-motion ball bushing

Liquid level

Extension stop

"O" ring seal

Orifice plate

Ski mounting bracket

Cylinder
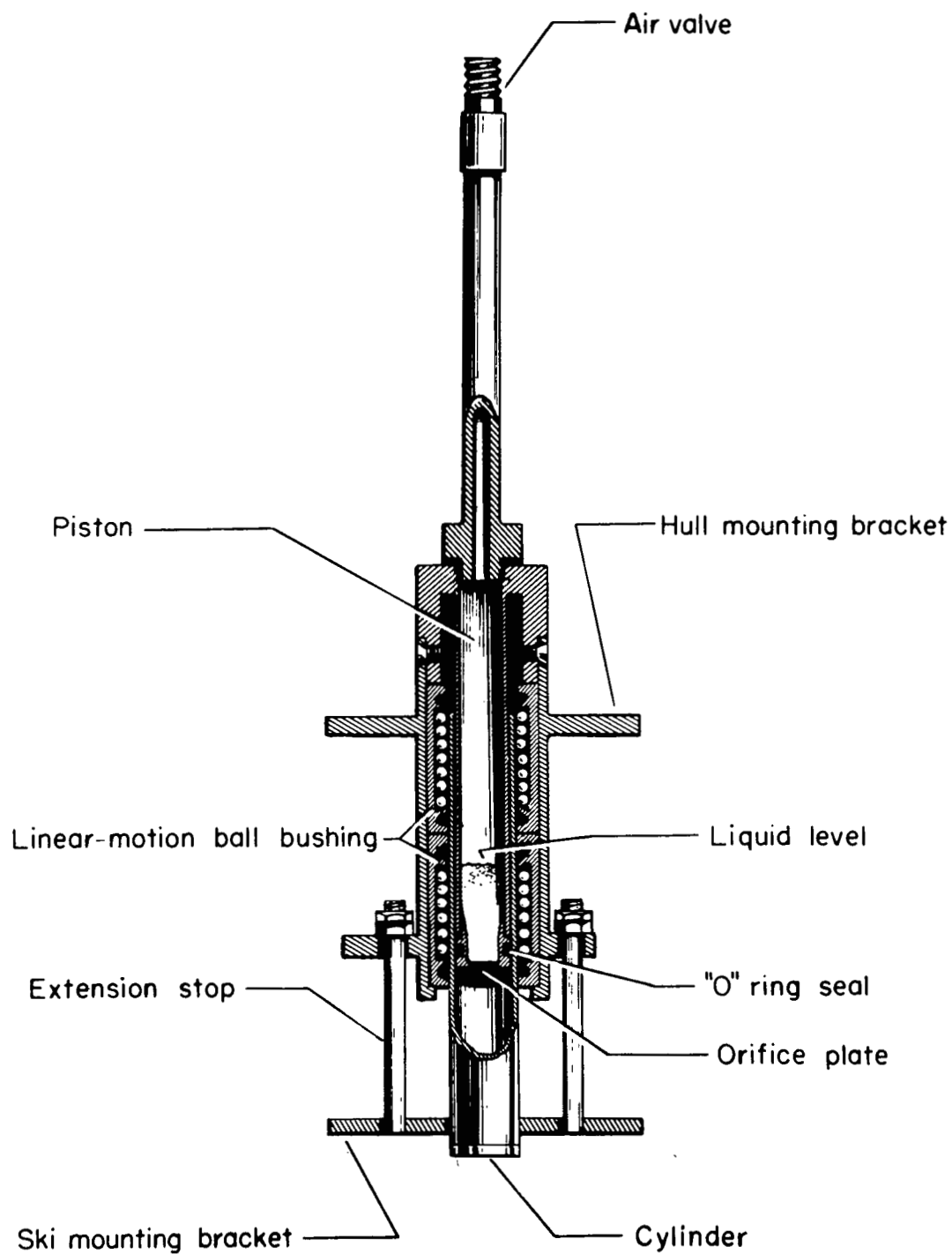
Figure 4.- Shock-absorber strut.

$$F_a = \frac{11.25}{1.5 - (z'-z)}$$
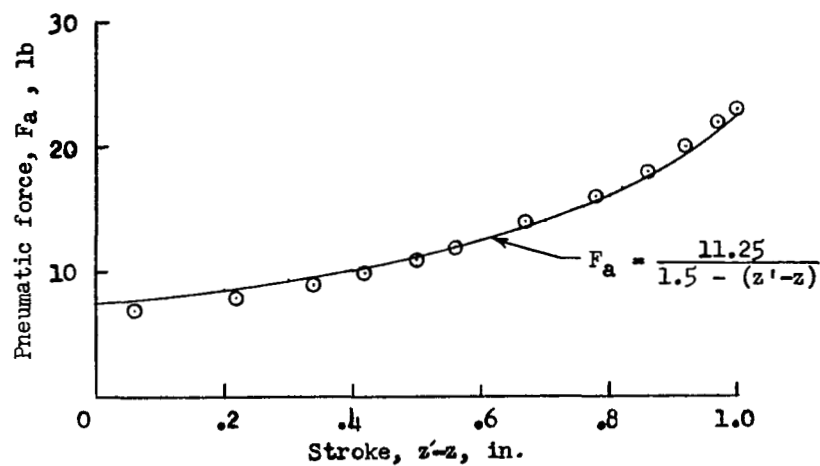
(a) Variation of pneumatic force with stroke.
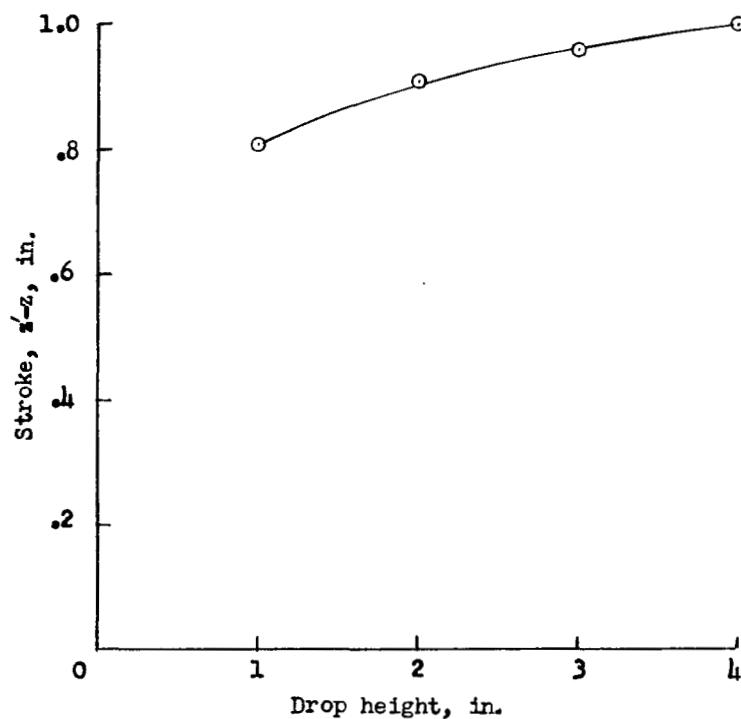
(b) Variation of stroke with drop height for a drop weight
of 11.57 pounds.

Figure 5.- Shock-absorber characteristics obtained
from bench tests.
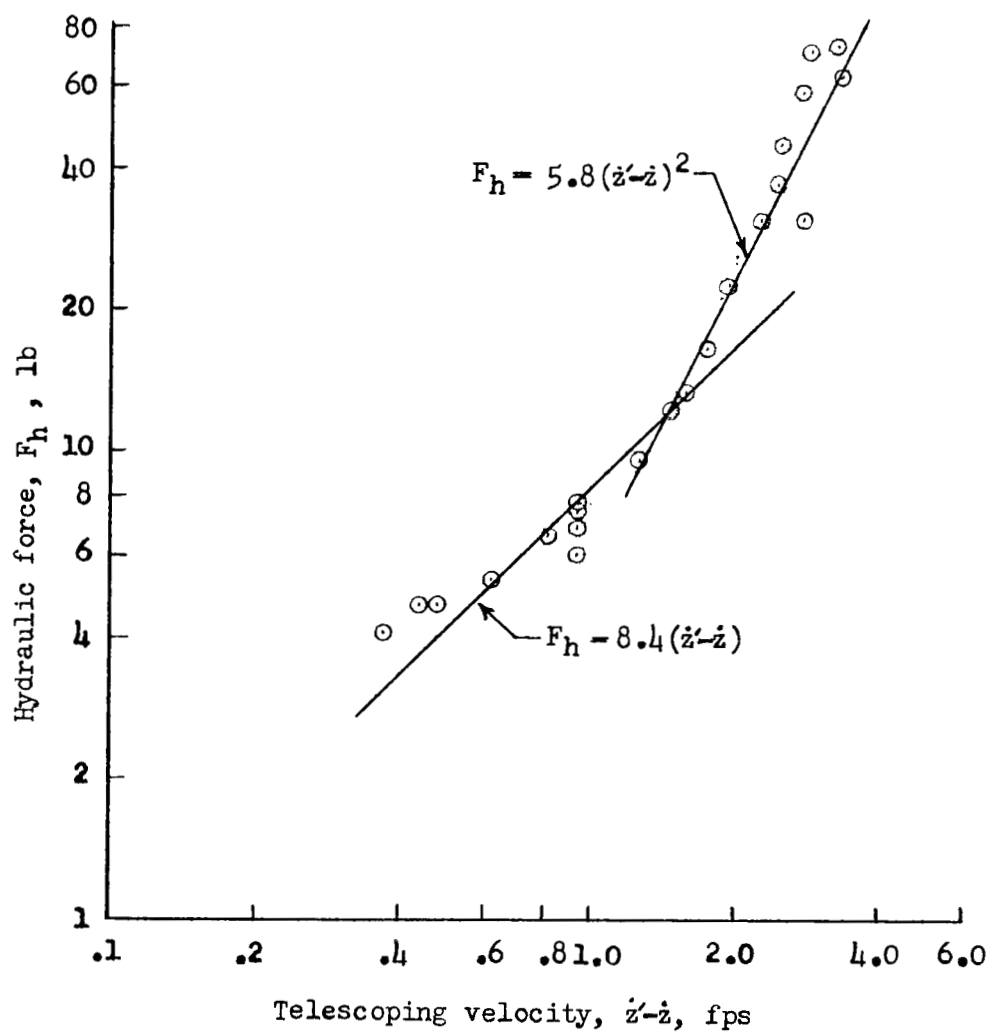
(c) Variation of hydraulic force with telescoping velocity. Drop
weight, 11.57 pounds; drop height, 4 inches.

Figure 5.- Concluded.

$\frac{1}{2}$"

10"

4"

Float detail

Fixed platform

Slide wire pickup

Water level

Float

4'
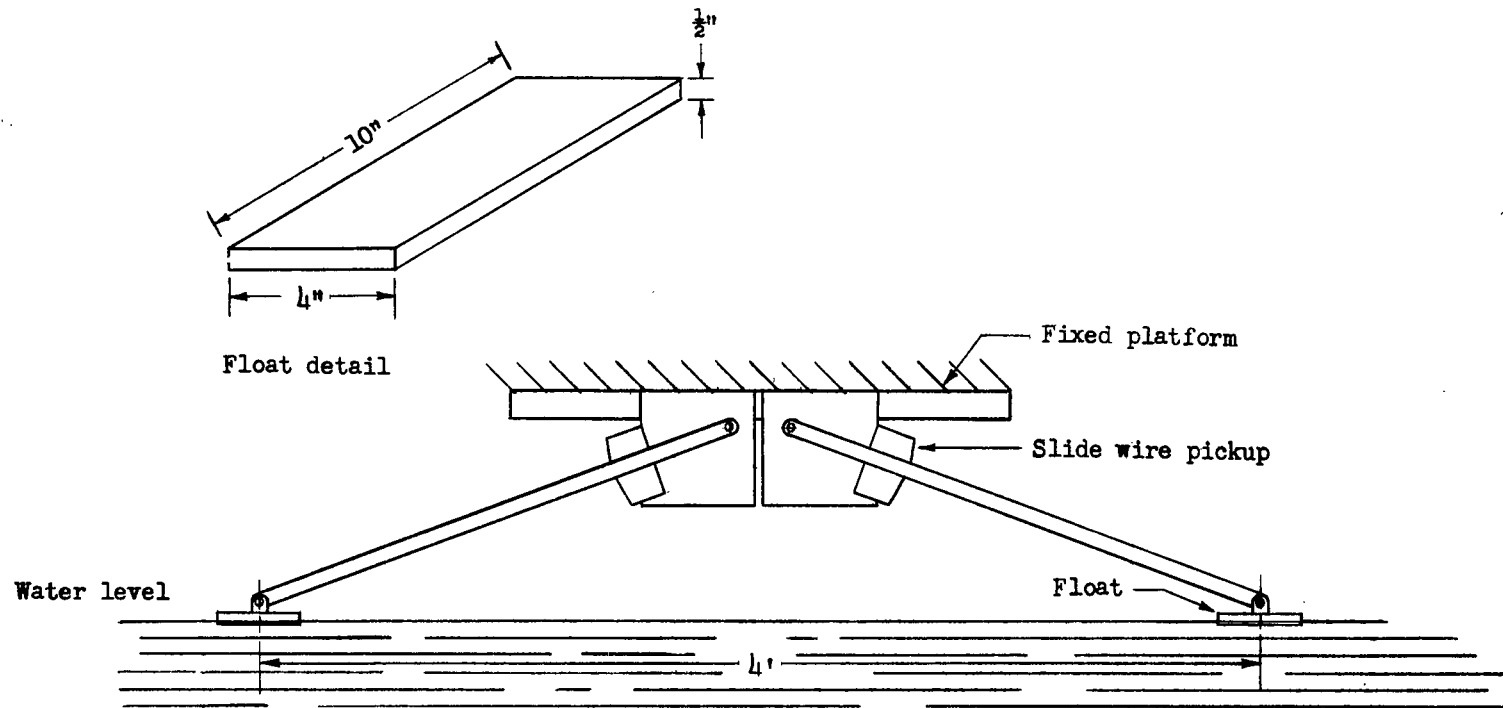
Figure 6.- Wave-recorder setup.
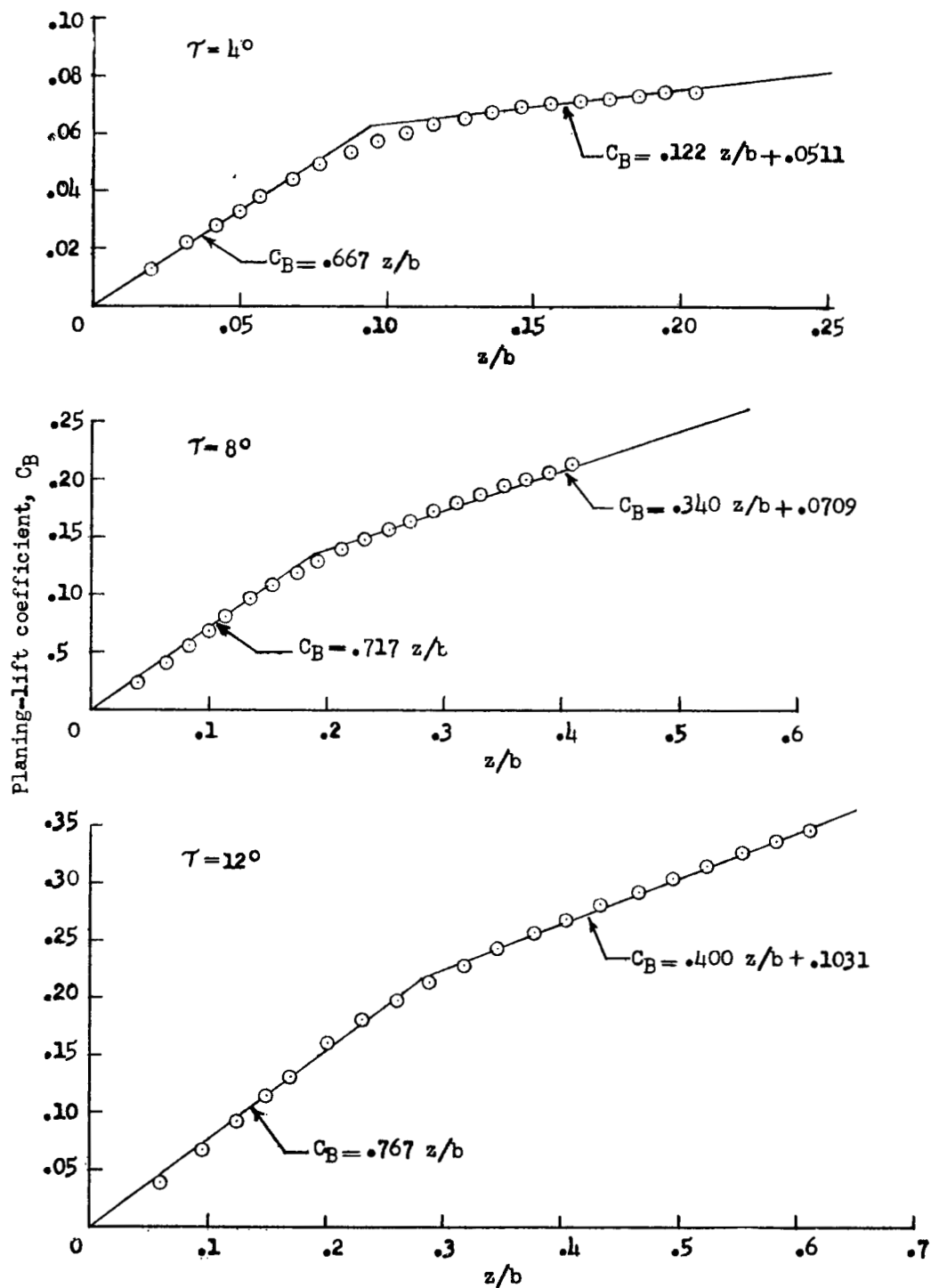
Figure 7.- Variation of planing-lift coefficient with draft in beams.

Figure 8.- Velocities and angles at contact on waves.
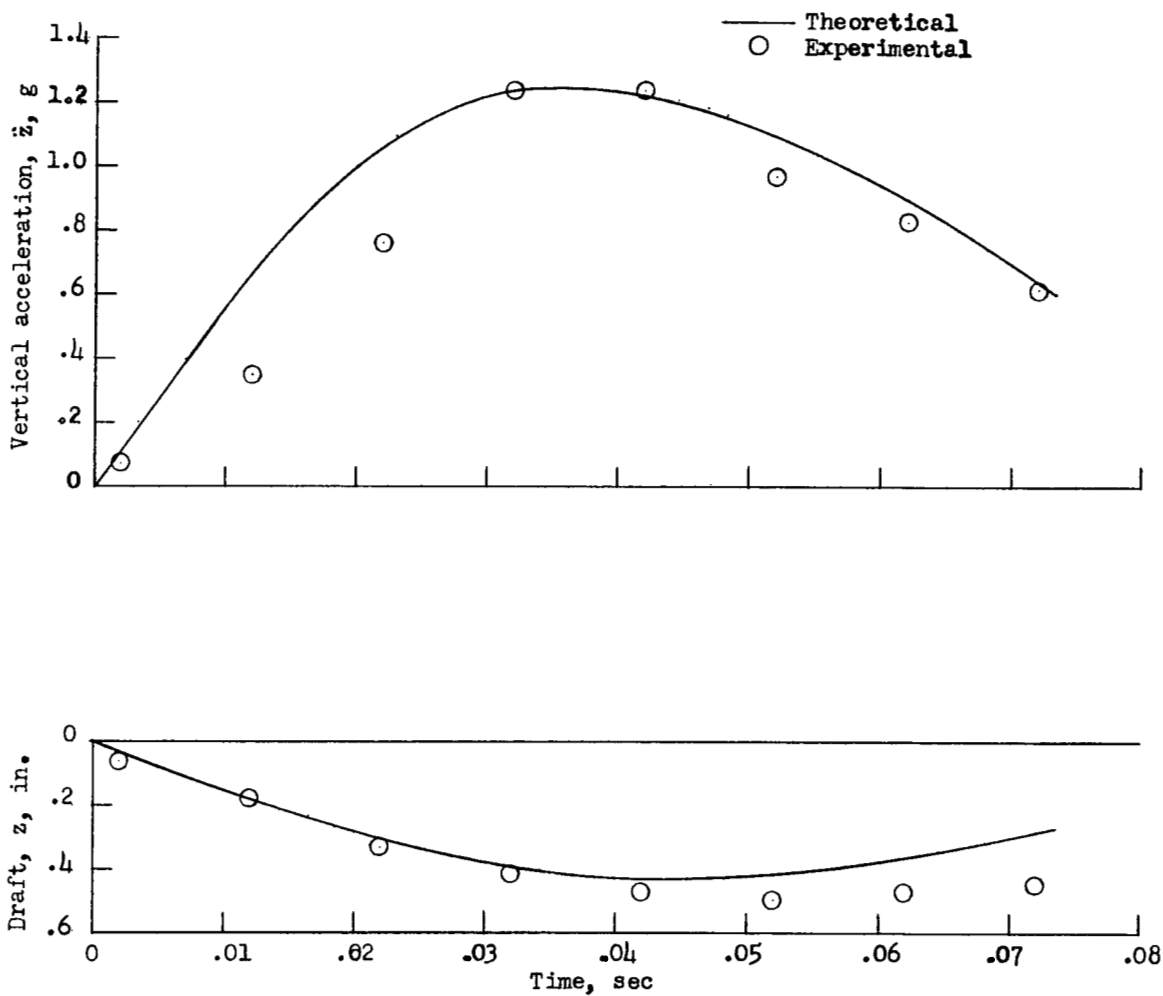
(a) Calm water; $\tau = 9.8^\circ$; $\gamma = 1.5^\circ$.

Figure 9.- Comparison of experimental and theoretical time histories for fixed-ski case.
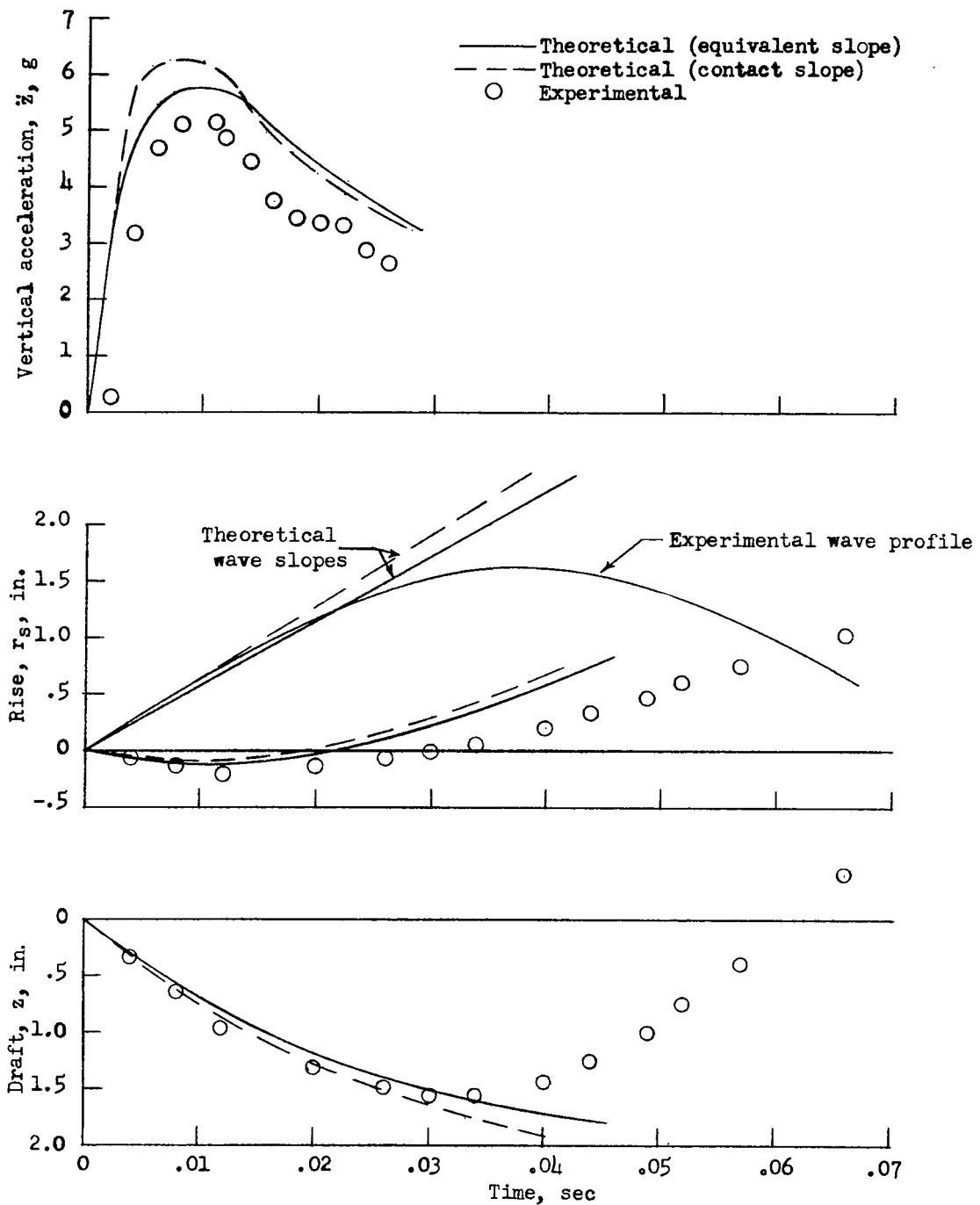
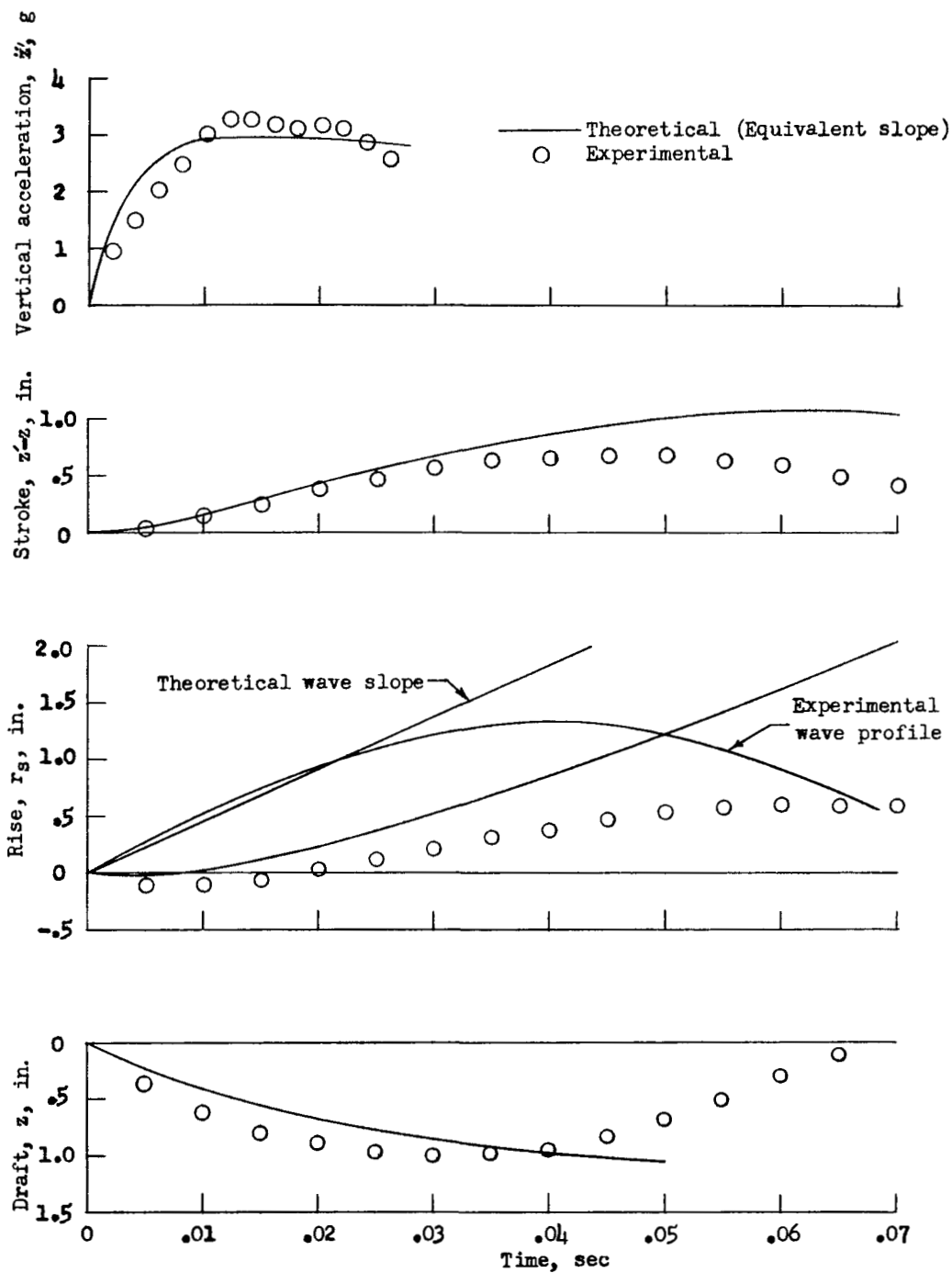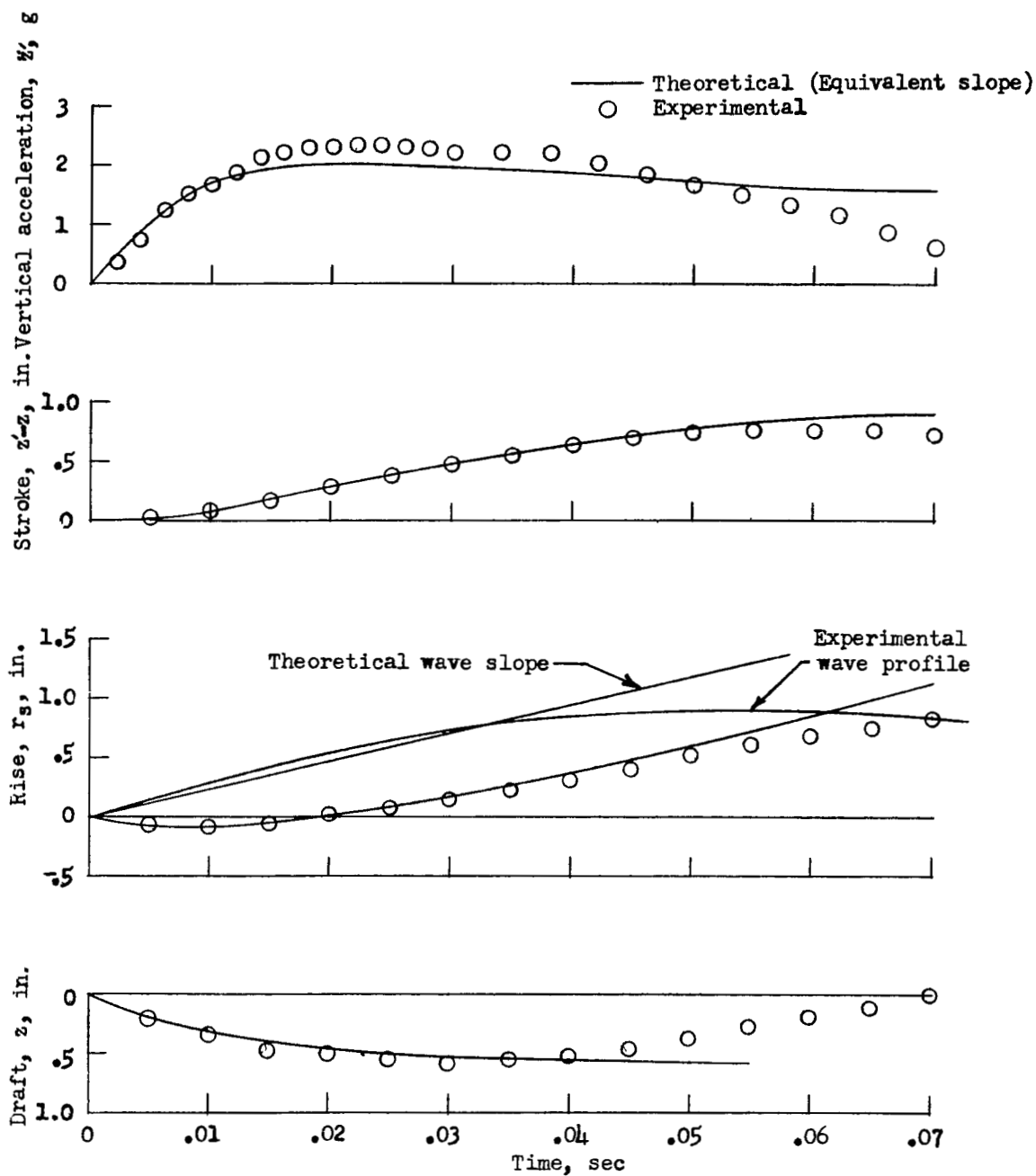(b)   H = 3.18 inches; L = 114 inches; τ = 9.1°; γ = 1.8°.

Figure 9.- Continued.
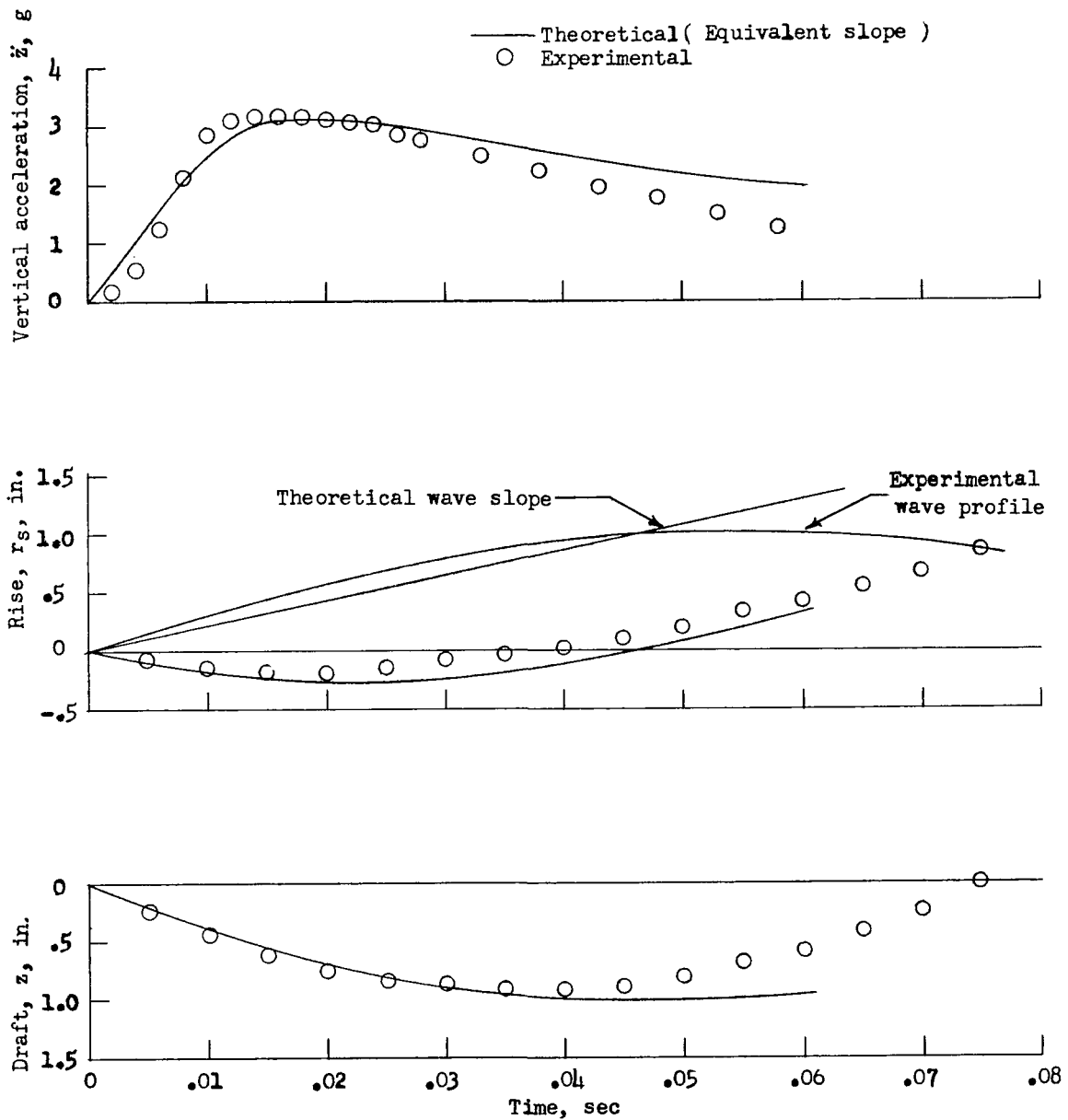
(c)   H = 2.94 inches; L = 220 inches; τ = 9.8°; γ = 1.8°.

Figure 9.- Concluded.
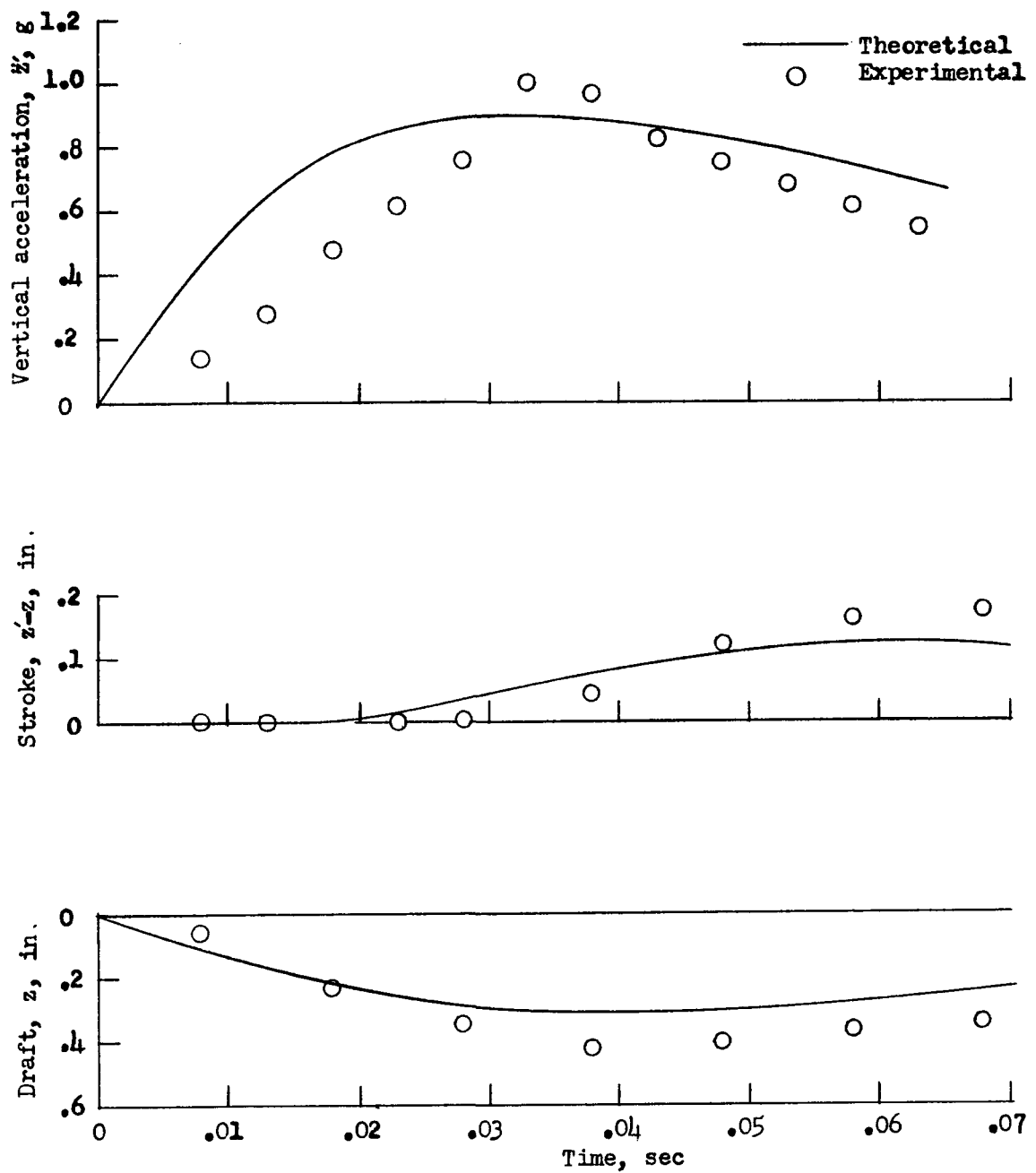
(a) Calm water; $\tau = 9.4°$; $\gamma = 1.4°$.

Figure 10.- Comparison of experimental and theoretical time histories
for translating-ski case.

(b) H = 2.58 inches; L = 118 inches; τ = 8.9°; γ = 2.0°.

Figure 10.- Continued.

(c)   H = 2.90 inches; L = 218 inches; τ = 9.0°; γ = 1.8°.

Figure 10.- Concluded.